

A Numerical Simulation of the Effect of Ambient Temperature on Capillary Tube Performance in Domestic Split Air Conditioners with R22 Alternatives

Khalid A. Joudi*, Qusay R. Al-Amir
Dept. Mech. Eng., Babylon Univ., Iraq
E-mail address: khalid47joudi@yahoo.com

Abstract

A numerical model has been formulated to simulate the capillary tube in split air conditioners of 1 and 2 TR capacities under high outdoor air temperatures. The outdoor air temperature was varied from 35 to 55°C with 5 °C increments. Three environment friendly refrigerants were used as alternatives to R22. They are R290, R407C and R410A. Finite difference method has been adopted in conjunction with EES software. This model is capable of predicting pressure, temperature, quality, velocity and viscosity distributions through the capillary tube for all refrigerants. The geometrical parameters and input conditions to the capillary tube model are extracted from experimental data. These include inner diameter, mass flow rate, surface roughness, temperature and pressure of the subcooled liquid refrigerant. The results show that the capillary choking length increases with increasing outdoor air temperature. Results of the simulation show that R290 needs more capillary length than the other refrigerants investigated, whereas R410A needs less capillary tube length.

Keywords: Capillary tube simulation; capillary tube with R22, R290, R407C, R410A; high ambient effect on capillary tube.

Highlights:

- Capillary tube characteristics at high ambient for R22 and Alternatives
- R290, R407C, R410A performance in capillary tubes at high ambient
- Capillary tubes simulation with R290, R407C, R410A in split A/C at high ambient.

1. Introduction

A capillary tube is a constant area expansion device, which is commonly used in low capacity systems such as domestic refrigerators, freezers, and room air conditioners because of its simplicity and low cost. The capillary tube creates the pressure drop between the high and low pressure sides.

In the past decades, most studies essentially focused on the flow through straight capillary tubes ([1],[2],[3],[4]). Jung et al. [1] performed experimental and theoretical studies of pressure drop through a capillary tube to predict the size of capillary tubes used in residential air conditioners and also to provide simple correlations for practicing engineers. The study covered condensing temperatures of 40 °C, 45 °C, 50 °C, and subcooling (0 °C, 2.5 °C, 5 °C), capillary tube diameter (1.2 - 2.4 mm), mass flow rate (5-50 g/s). The results indicated that the capillary tube length varies uniformly with the changes in condensing temperature and subcooling.

Kim et al. [2] discussed the characteristics of flow and pressure drop in adiabatic capillary tubes of inner diameters of 1.2 to 2.0 mm, and tube lengths of 500 to 2000 mm for several condensing temperatures and various degrees of subcooling with R22.

A numerical simulation of straight capillary tube was carried out by Imran [3] for R22 and alternative R407C. Zhou and Zhang [4] investigated the performance of coiled adiabatic capillary tubes both theoretically and experimentally. They developed a new method including metastable liquid and two phase regions.

The main objective of this study is to study the effect of ambient temperature on coiled capillary tubes in domestic split air conditioners with ozone friendly refrigerants under high outdoor air temperatures.

2. ADIABATIC CAPILLARY TUBE MODELING

The refrigerant flow inside the capillary tube can be divided into single phase and two-phase regions. **Fig.(1)** is a schematic diagram of the coiled capillary tube where point 1 denotes the condenser exit and point 2 is the capillary tube inlet. There is a small pressure drop between these points due to entrance loss. The refrigerant enters the capillary tube at point 2 as a subcooled liquid. The pressure decreases linearly until the refrigerant becomes saturated liquid at point 3. Beyond point 3, the refrigerant enters the two phase region where the pressure decreases non-linearly with length until it reaches the end of the capillary tube at point 4. Finally, point 5 represents the evaporator inlet.

The present model uses the following assumptions:

1. The capillary tube operates at steady state.

2. A subcooled liquid enters the capillary tube .
3. The flow of refrigerant inside the capillary tube is one dimensional, homogenous and adiabatic.
4. Changes in kinetic and potential energies are negligible.
5. Isenthalpic expansion through the capillary tube.

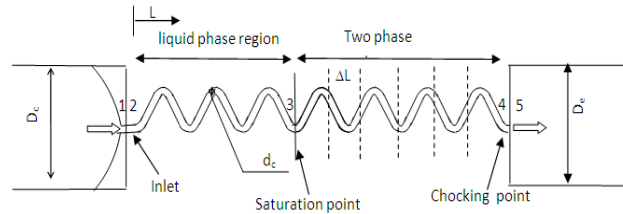


Fig.1 Schematic diagram of a capillary tube

Applying the Bernoulli equation between points 1 and 2, the minor pressure drop at the entrance was calculated by Sinpiaboon and Wongwises [5] as;

$$P_1 - P_2 = (1 + k) \frac{\rho V^2}{2} \quad (1)$$

Where k is the entrance loss factor. References are not in agreement about its value. The value of $k=0.5$ is used here as given by Chen [6].

In the single phase region between points 2 and 3, the pressure at point 2 decreases linearly until saturation pressure at point 3 according to the following equation (Munson and Young [7]);

$$P_2 - P_3 = f_s \frac{L_s}{d_{ca}} \frac{\rho V^2}{2} \quad (2)$$

The single phase length L_s is calculated from substituting equation 2 in equation 1 (Sukkarin and Somchai[8]) thus;

$$L_s = \frac{d_{ca}}{f_s} \left[\frac{2\rho}{G^2} (P_1 - P_3) - (k + 1) \right] \quad (3)$$

where G is the mass velocity and f_s is the friction factor, which can be determined from the Moody correlation (Moody [9]).

$$f_s = \frac{1.325}{\left[\ln \left(\frac{e/d_{ca}}{3.7} + \frac{5.74}{Re^2} \right) \right]^2} \quad (4)$$

By applying the steady flow energy equation for the single phase liquid region in the capillary tube with negligible work and heat exchange, we get:

$$H_2 = H_3 = H_s \quad (5)$$

Applying the steady flow energy equation for each element lying in the two phase region, between points 3 and 4:

$$H_3 + \frac{V_3^2}{2} = H_f + x H_{fg} + \frac{G^2}{2} (v_f + x v_{fg})^2 \quad (6)$$

Equation 6 is quadratic in x and the quality x can be expressed as ;

$$x = \frac{-H_{fg} - G^2 v_f v_{fg} \mp \sqrt{(G^2 v_f v_{fg})^2 - 2G^2 v_{fg}^2 \left(\frac{G^2 v_f^2}{2} - H_3 - \frac{V_3^2}{2} + H_f \right)}}{G^2 v_{fg}^2} \quad (7)$$

Once the quality for element i is known, properties such as viscosity, density and entropy can be easily calculated by using the saturated properties for the liquid and vapor phases as:

$$\mu_i = x_i \mu_{g,i} + (1 - x_i) \mu_{f,i} \quad (8)$$

$$\rho_i = \left(\frac{x_i}{\rho_{g_i}} + \frac{(1-x_i)}{\rho_{f_i}} \right)^{-1} \quad (9)$$

$$s_i = x_i s_{g_i} + (1-x_i) s_{f_i} \quad (10)$$

The Reynolds number in the two phase region is determined as:

$$Re_i = \frac{\rho_i V_i d_{ca}}{\mu_i} \quad (11)$$

Where V_i is the velocity for element i in the two phase region. The two phase friction factor f_i is calculated by the correlation given by Sami and Tribes [10];

$$f_i = \frac{3.1}{\sqrt{Re_i(1-x_i)}} \exp\left[\frac{(1-x_i)^{0.25}}{2.4}\right] \quad (12)$$

The incremental length of each section in the two-phase region is calculated as follows(Sukkarin and Somchai,[11]):

$$\Delta L_i = \frac{2d_{ca}}{f_i} \left[\frac{-\rho_i \Delta P}{G^2} + \frac{\Delta \rho}{\rho_i} \right] \quad (13)$$

The calculation in two phase flow region is terminated when the flow approaches the choked. The total length of the two-phase region is;

$$L_t = \sum_{i=2}^n \Delta L_i \quad (14)$$

Finally, the total length of the capillary tube is the sum of the single phase and two-phase lengths, i.e.

$$L_{tot} = L_s + L_t \quad (15)$$

The coiling effect of the capillary tube can be entered in the calculation of the friction factors. A straight tube model can also be applied to coiled capillary tubes by changing the corresponding friction factor equations (Sukkarin and Somchai,[11]). The equation proposed by Mori and Nakayama [12] is used here with different coefficients for the tube coiled wall roughness as;

$$f_c = \frac{C_1 (d_{ca}/D_c)^{0.5}}{[Re (d_{ca}/D_c)^{2.5}]^{1/16}} \left\{ 1 + \frac{C_2}{[Re (d_{ca}/D_c)^{2.5}]^{1/16}} \right\} \quad (16)$$

Where:

$$C_1 = 1.88411177 * 10^{-1} + 85.2472168(e/d_{ca}) - 4.63030629 * 10^4 (e/d_{ca})^2 + 1.31570014 * 10^7 (e/d_{ca})^3$$

$$C_2 = 6.79778633 * 10^{-2} + 25.388038(e/d_{ca}) - 1.0613314 * 10^4 (e/d_{ca})^2 + 2.54555343 * 10^6 (e/d_{ca})^3 \quad \dots\dots(17)$$

This method is used for both liquid and two phase regions.

3. SOLUTION PROCEDURE

The Engineering Equation Solver (EES) software(Klein [13]) is used in this work for computer programming. Refrigerant thermo-dynamic and transport properties such as density, dynamic viscosity, specific enthalpy, thermal conductivity are taken from EES software. In the single-phase region, after calculating the Reynolds number, the single phase friction factor and single phase length were calculated. Initial condition of two phase region is the end condition of the single phase flow region. Calculation of the two-phase region length L_r required a numerical solution due to the change in quality along this region (see Eq.7). For each element in the two-phase region, the pressure P_i , the temperature T_i , the vapor quality x_i , the entropy S_i and the two-phase friction factor (f_i) were calculated. At each element, the calculated entropy S_i was compared with the entropy of the previous element S_{i-1} , to make sure that the entropy increased as the refrigerant flows through the capillary tube. The entropy increases continuously through the capillary tube to a certain maximum and then it begins to decrease (choking condition). The two phase region length is calculated by eq.(14). The total capillary tube length is the

sum of the two region lengths.

Fig. 3 shows the flow chart of simulation model for the capillary tube .

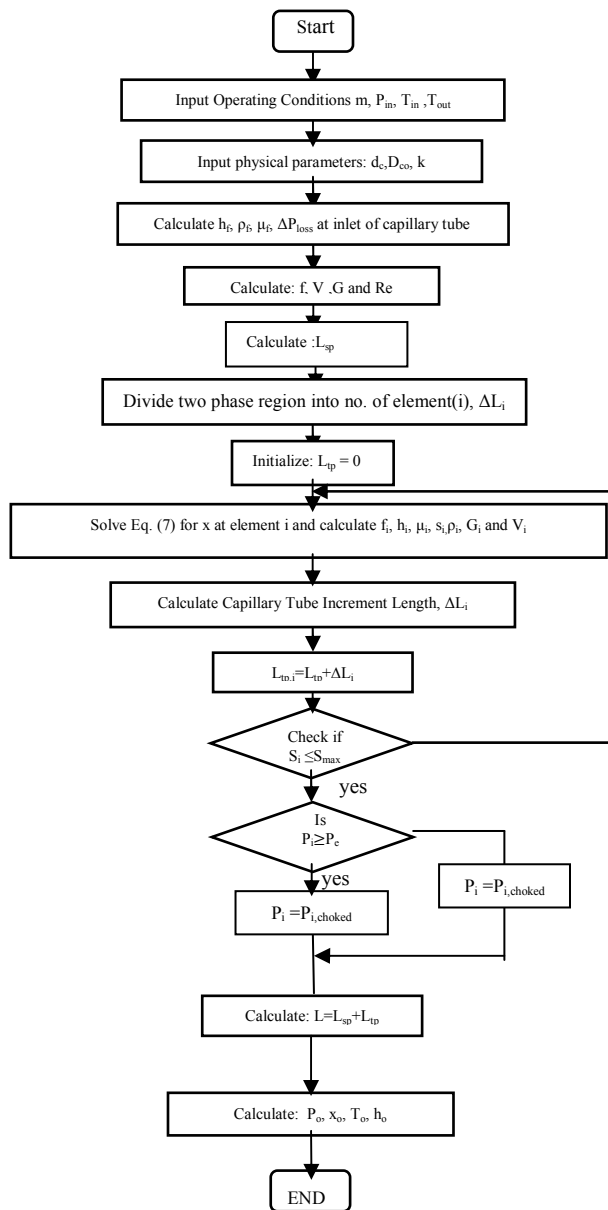


FIG. 2. SIMULATION MODEL FLOW CHART FOR THE CAPILLARY TUBE

4. RESULTS AND DISCUSSION

Fig.3 compares the pressure distribution along the capillary tube in the present study and that of Sukkarin et al.[8]. The comparison is good. Only R22 and R410A results are shown as typical results. The present model can be used to predict the flow characteristics for the other alternatives.

Fig.4 shows the pressure distribution along the capillary tube at ASHARE standard test conditions for 1 TR and 2 TR systems. For an actual cycle, each refrigerant has a different condensing temperature and pressure. Therefore, the capillary tube length is different for each one. The capillary tube length depends on the operating conditions at the inlet of the capillary tube and thermo-physical properties, especially viscosity, of the refrigerant. It is observed that there is a linear drop in pressure for R22 and its alternatives between the entrance of the capillary tube and saturation (flash) point in the single phase region. The pressure drops rapidly near the end of the tube in the two phase region. Results showed that R290 required more length for choking due to its lower liquid viscosity and refrigerant mass flow rate than the other refrigerants tested. R410A needed less. The magnitude of pressure drops is different for each refrigerant depending on its mass flow rate (or its specific volume). Thus, R290 shows the lowest pressure drops owing to its large specific volume. Whereas, the similar specific volumes of R22 and

R407C make their pressure drops similar. R410A has the largest pressure drop. This is true for both systems. The change in vapor quality with length of the capillary tube is shown in Fig.5. For all refrigerants, the quality is zero up to the flash point. After that, the change of vapor quality increases sharply towards the end of the tube in the two phase region. The reason for this behavior is that the acceleration and friction effects in the two-phase region increase the pressure gradient giving rise to a higher vaporization rate. Fig. 6 shows the temperature distribution along the capillary tube at standard conditions for the 1 TR and 2 TR systems. The temperature drop, of all refrigerants is insignificant in the single phase region. However, in the two-phase region, the temperature drops sharply with pressure.

The Reynolds number along the capillary tube at standard conditions for R22 and its alternatives for both 1 TR and 2 TR systems is shown in Fig.7. In the single phase region, the variations of Reynolds number is minimal because the thermo-physical properties of the liquid refrigerant do not change significantly. In the two phase flow, the values of Reynolds number start to drop because the thermo-physical properties, especially the viscosity, increases as the capillary tube length increases. The velocity distributions along the capillary tube at standard conditions for the two systems is shown in Fig.8. In the single phase region, the velocity remains constant because the refrigerant remains liquid. In the two phase region, the flow velocity of refrigerant increases because of the specific volume of the mixture increases due to vaporization.

Figs.9 and 10 show the effect of outdoor air temperature on pressure distribution along the capillary tube for R22 and R410A as typical results. As the outdoor air temperature increases, the condenser pressure and mass flow also increase. This increases both the single phase and two phase lengths. Therefore, the total length of the capillary tube for R22 refrigerant increased from 1.78 m to 2.69 m as the outdoor air temperature increased from 35°C to 55°C. For R410A, it increased from 1.29 m to 2.43 m.

Fig 11 shows the vapor quality along the capillary tube as a function of outdoor air temperatures for R290 as a typical result. When the outdoor air temperature increases, the quality values at exit increase due to the increase of the specific volume of the mixture. Fig.12 shows a typical temperature distribution along the capillary tube as a function of outdoor air temperatures for R407C. As the outdoor air temperature increases, the condensing temperature at the entrance to the capillary tube increases. The capillary tube length increases accordingly with the condensing temperature. Extensive details for all four refrigerants are given by Al-Amir [17].

5. CONCLUSIONS

1. R290 required the longest capillary tube length due to its lower liquid viscosity and mass flow rate than the other refrigerant. R410A needed the shortest length.
2. The magnitude of pressure drops is different for each refrigerant. R290 showed the smallest pressure drop. Similar specific volumes of R22 and R407C made their pressure drops similar. R410A showed the largest pressure drop across the capillary tube.
3. Increasing the outdoor air temperature, increases the condenser pressure for all refrigerants. This increased both the single phase and two phase lengths.

REFERENCES

- [1] Jung D., Park C., Park P., 1999, " Capillary tube selection for HCFC22 alternative", International Journal of Refrigeration 22, 604-614.
- [2] Kim S. G., Kim M. S., Ro S.T., 2001, " Flow and Pressure Drop Characteristics of R22 In Adiabatic Capillary Tubes" KSME International Journal; Vol. 15 No.9, pp. 1328-1338.
- [3] Imran A. A. , 2009, " Adiabatic and Separated Flow of R-22 and R-407C in Capillary Tube", Eng & Tech. Journal , Vol .27, No 6.
- [4] Zhou G., Zhang Y., 2006, " Numerical and experimental investigations on the performance of coiled adiabatic capillary tubes", Applied Thermal Engineering 26, 1106–1114.
- [5] Sinpiboon J. , Wongwises S., 2002, " Numerical investigation of refrigerant flow through non-adiabatic capillary tubes" Applied Thermal Engineering , 22, 2015–2032.
- [6] Chen W., 2008, " A comparative study on the performance and environmental characteristics of R-410A and R-22 residential air conditioners", Applied Thermal Engineering , Vol. 28, 1-7.
- [7] Munson B. R., Young D. F., 2010, " Fundamentals of Fluid Mechanics" Fourth edition, John Wiley & Sons. Inc. USA.
- [8] Sukkarin C., Somchai W., 2010, " Effects of coil diameter and pitch on the flow characteristics of alternative refrigerants flowing through adiabatic helical capillary tubes" International Communications in Heat and Mass Transfer 37, 1305–1311.
- [9] Moody, L.F., Friction Factors for Pipe Flow, ASME, Vol. 66, pp. 671-684, 1944.
- [10] Sami S. M. and Tribes C., 1998, "Numerical Prediction of Capillary Tube Behavior with Pure and Binary Alternative refrigerants", Journal of Applied Thermal Engineering, Vol. 18, No 6, P.491-502.
- [11] Sukkarin C., Somchai W., 2011, " A comparison of flow characteristics of refrigerants flowing through

adiabatic straight and helical capillary tubes" International Communications in Heat and Mass Transfer 38, 398–404.

[12] Mori Y., Nakayama W., 1967, "Study on forced convective heat transfer in curve pipes II", International Journal of Heat and Mass Transfer, Vol.10, No.1, 37–59. Quoted by Sukkarin et al.,2011.

[13] Klein S.A., 2006, Engineering Equation Solver commercial version V8.914 .

[14] G. Bo, L. Yuanguang, W. Zhiyi, J. Buyun, Analysis on the adiabatic flow of R407C in capillary tube, Appl. Therm. Eng. 23 (2003) 1871–1880

[15] J.L. Hermes , M. Cludio, T. K. Fernando, Algebraic solution of capillary tube flows. Part II: Capillary tube suction line heat exchangers, Appl. Therm. Eng. 30 (2010) 770–775

[16] P.K. Bansal , G. Wang, Numerical analysis of choked refrigerant flow in adiabatic capillary tubes, Appl. Therm. Eng. 24 (2004) 851–863

[17] Al-Amir Q. R., 2013, " Experimental assessment and numerical simulation of the performance of small scale air-conditioning systems using alternative refrigerants to R-22", PhD thesis, College of Engineering, University of Baghdad.

NOMENCLATURE

D	Coiling Diameter(m)	-
d	Capillary tube inner diameter (m)	-
e	Roughness (m)	-
f	Friction factor	-
G	Mass flux(kg/s.m ²)	-
H	Enthalpy(kJ/kg)	-
K	Thermal conductivity(W/m.K)	-
k	Entrance loss factor	-
L	Length (m)	-
P	Pressure(N/m ²)	-
Re	Reynolds number	-
S	Entropy (kJ/kg.k)	-
V	Velocity(m/s)	-
v	Specific volume(m ³ /kg)	-
x	Vapor quality	-

Greek Symbols

Δ	Change
μ	Dynamic viscosity (kg/m's)
ρ	Density (kg/m ³)

Subscripts

c	condenser
capillary	
e	evaporator
single phase	
two phase	
liquid	
g	vapor
element	

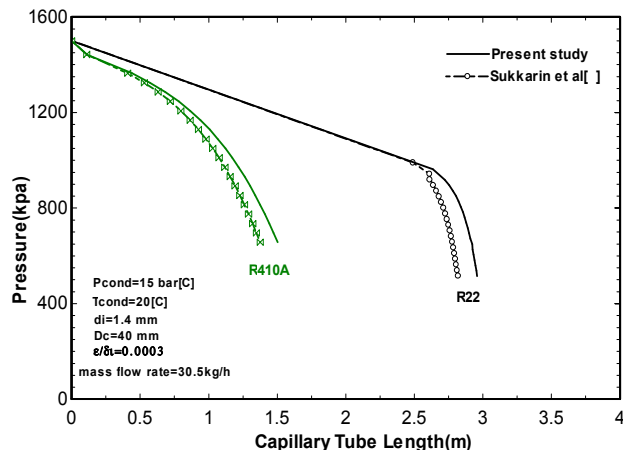
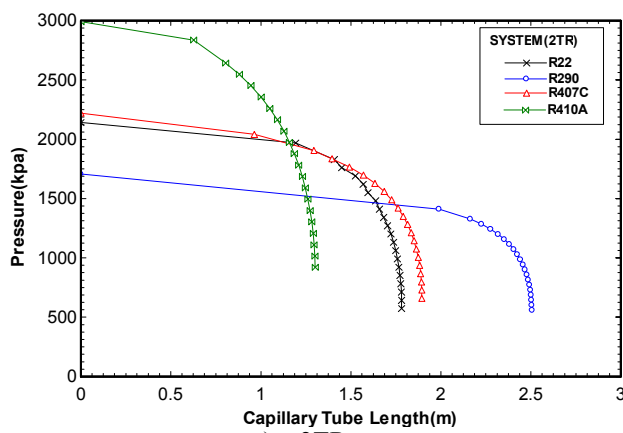
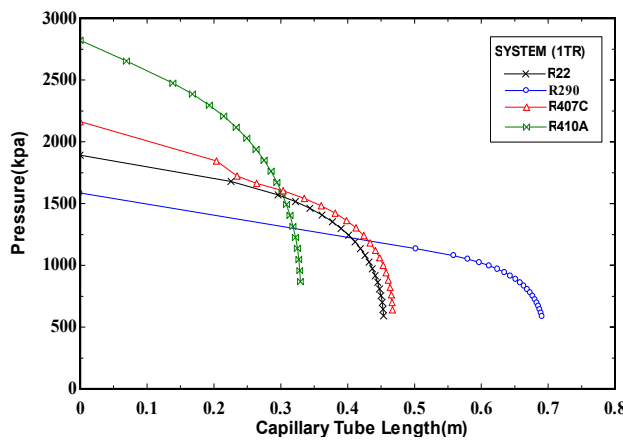


Fig.3 Pressure distribution along the capillary tube.



a) 2TR system



b) 1TR system

Fig.4 Pressure distribution along the capillary tube at standard test conditions for 1 TR and 2 TR systems .

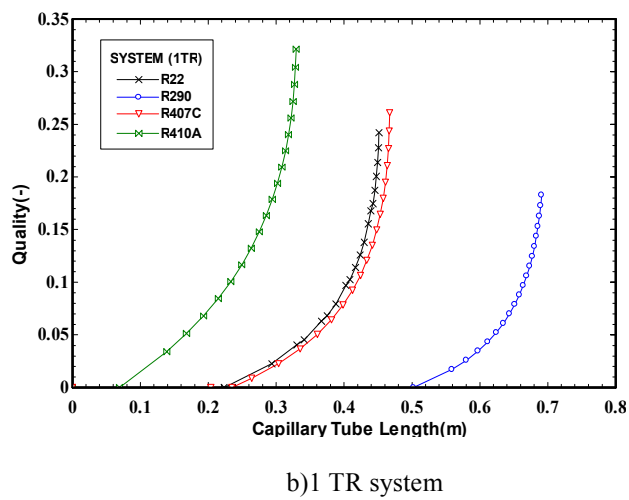
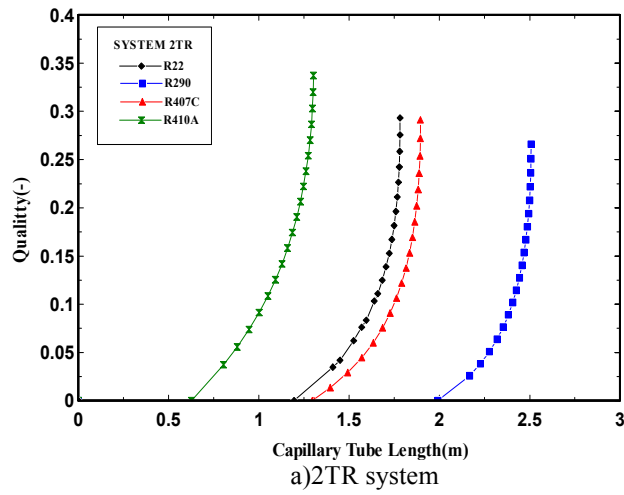
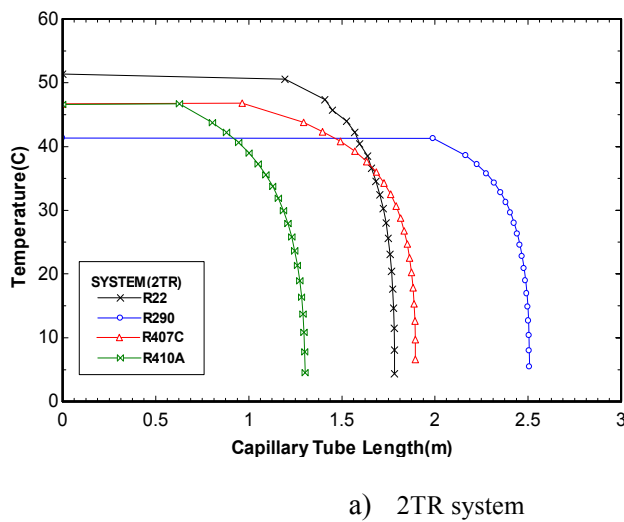
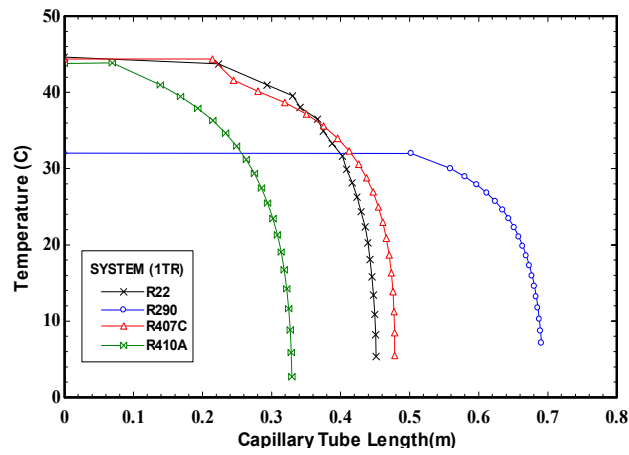


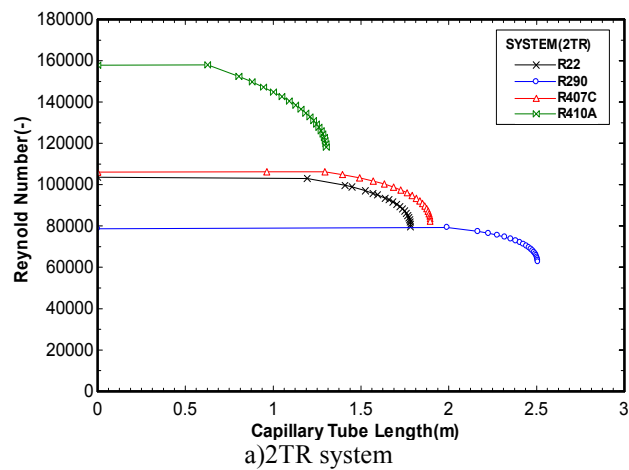
Fig.5 Quality distributions along the capillary tube at standard conditions for 1 TR and 2 T Rsystems.



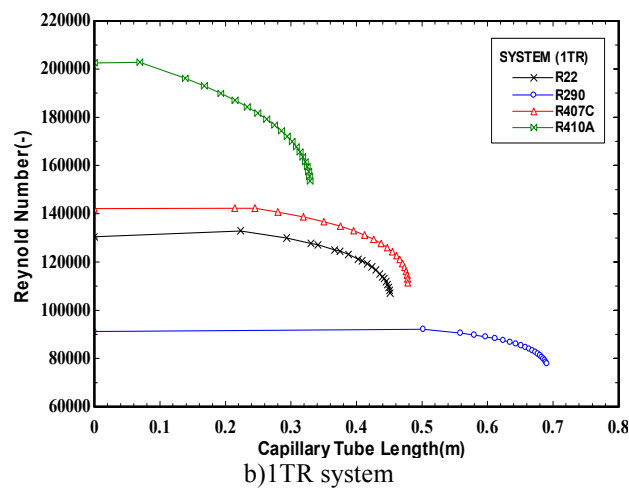


b)1TR system

Fig.6 Temperature distributions along the capillary tube at standard conditions for 1 TR and 2 T R systems .



a)2TR system



b)1TR system

Fig.7 Reynolds numbers along the capillary tube at standard conditions for 1 TR and 2 T R systems.

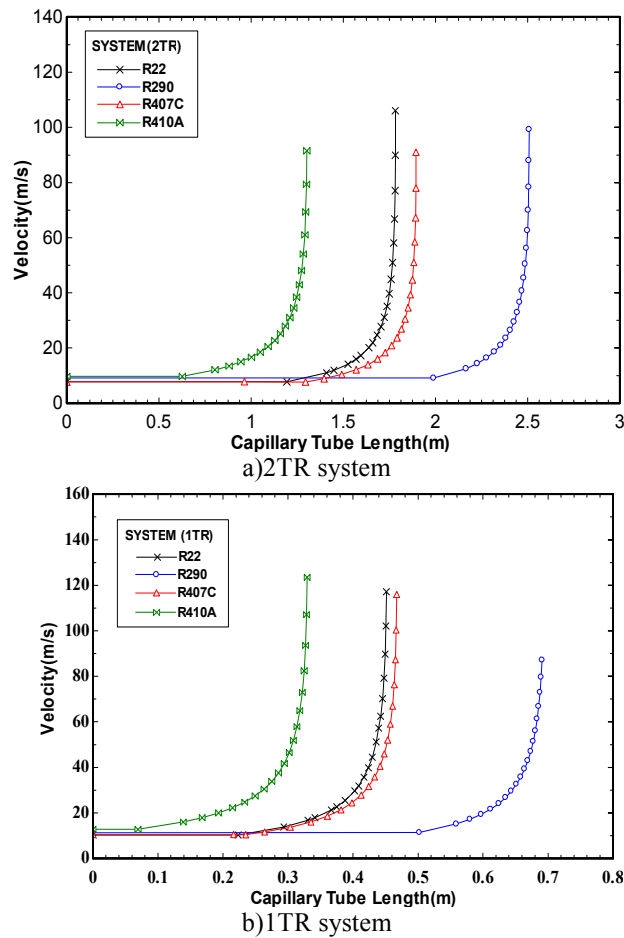


Fig.8 Velocity distributions along the capillary tube at standard conditions for 1 TR and 2 T Rsystems .

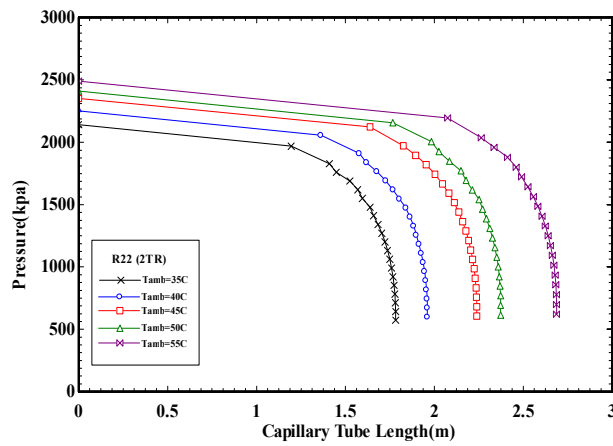


Fig.9 Pressure distribution along the capillary tube at different outdoor air temperature for R22

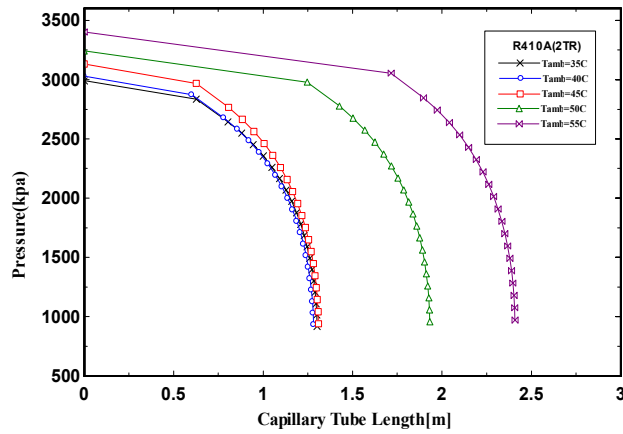


Fig.10 Pressure distribution along the capillary tube at different outdoor air temp. for R410A

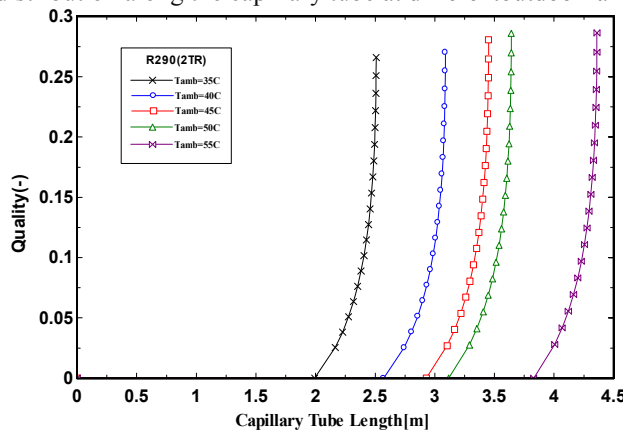


Fig.11 Quality distribution along the capillary tube at different outdoor air temperature for R290

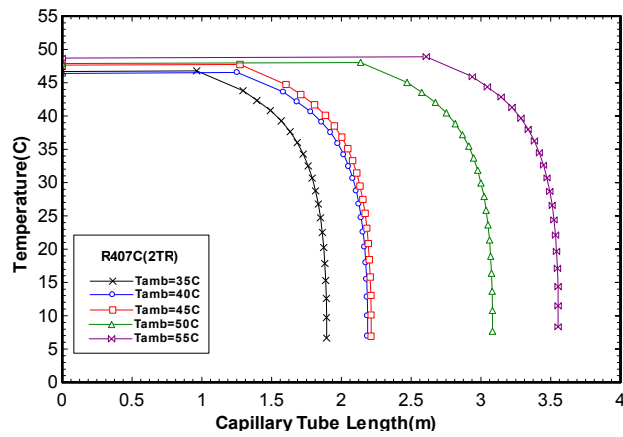


Fig.12 Temperature distribution along the capillary tube at different outdoor air temperature for R407C